PHILOSOPHICAL TRANSACTIONS A

rsta.royalsocietypublishing.org

Review

Cite this article: Meech KJ. 2017 Setting the scene: what did we know before Rosetta? *Phil. Trans. R. Soc. A* **375**: 20160247.
http://dx.doi.org/10.1098/rsta.2016.0247

Accepted: 6 March 2017

One contribution of 14 to a discussion meeting issue 'Cometary science after Rosetta'.

Subject Areas:
solar system

Keywords:
comets, solar system formation, Rosetta mission

Author for correspondence:
K. J. Meech
e-mail: meech@ifa.hawaii.edu

Setting the scene: what did we know before Rosetta?

K. J. Meech

Institute for Astronomy, 2680 Woodlawn Drive, Honolulu, HI 96822, USA

KJM, 0000-0002-2058-5670

This paper provides an overview of our state of knowledge about comets prior to the Rosetta mission encounter. Starting with the historical perspective, this paper discusses the development of comet science up to the modern era of space exploration. The extent to which comets are tracers of solar system formation processes or preserve pristine interstellar material has been investigated for over four decades. There is increasing evidence that in contrast with the distinct dynamical comet reservoirs we see today, comet formation regions strongly overlapped in the protoplanetary disc and there was significant migration of material in the disc during the epoch of comet formation. Comet nuclei are now known to be very low-density highly porous bodies, with very low thermal inertia, and have a range of sizes which exhibit a deficiency of very small bodies. The low thermal inertia suggests that comets may preserve pristine materials close to the surface, and that this might be accessible to sample return missions.

This article is part of the themed issue 'Cometary science after Rosetta'.

1. Historical understanding

Comets have not always enjoyed enthusiastic attention owing to their often sudden appearance and brightening, disturbing the regular harmony of the heavens. Early accounts of comets showed that they were often considered ill omens. Bright comets that are easily noticed by the public, however, are quite rare, having appeared in the historic record at a rate of about 2 per century on average over the past 2000 years (figure 1*a*).

A significant increase in comet observations occurred beginning in the 1600s (figure 1*b*,*c*) during the Renaissance energized by the transformation in scientific thinking brought about by the seventeenth century

THE ROYAL SOCIETY PUBLISHING

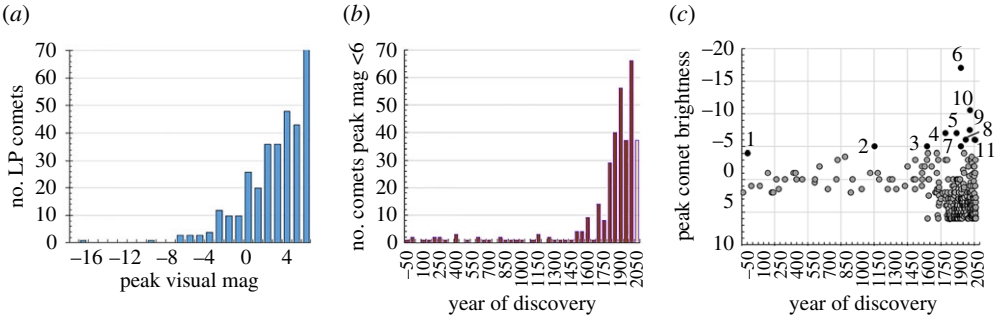

Figure 1. Historical discovery dates and observations of 337 bright naked eye visible ($V < 6$ mag) comets. Data are compiled from [1–3], from the D.K. Yeomans Web page summarizing great comets in history (http://ssd.jpl.nasa. gov/?great_comets), the summary of the brightest comets since 1935 compiled by the *International Comet Quarterly* (http://www.icq.eps.harvard.edu/brightest.html), Seiichi Yoshida's comet observation webpage (http://www.aerith.net/index.html) and the German comet group Web archive (http://kometen.fg-vds.de/fgk_hpe.htm). (*a*) Statistically, very bright 'great' comets ($V < 0$) were rare, with only 47 comets recorded over approximately 2100 years—a rate of approximately 2 comets per century. (*b*) The rate of discovery increased dramatically during the seventeenth century scientific revolution. (*c*) The distribution of bright comets versus discovery year shows that recently we have enjoyed a large number of notable comets. Comets brighter than $V \sim -5$ include: (1) C/-43 K1 (Caesar's comet); (2) X/1106 X1, the Great comet of 1106; (3) C/1577 V1, the Great comet of 1577 (Tycho's comet); (4) C/1743 X1, the Great comet of 1744; (5) C/1843 D1, the Great comet of 1843; (6) C/1882 R1, the Great comet of 1882; (7) C/1882 F1 (Wells); (8) C/1927 X1 (Skjellerup-Maristany); (9) C/1962 C1 (Seki-Lines); (10) C/1965 S1 (Ikeya-Seki); (11) C/2006 P1 McNaught and C/2011 W3 Lovejoy. (Online version in colour.)

scientific revolution and the work of Copernicus, Galileo, Brahe and Kepler. A first key piece of comet science occurred as a result of Tycho Brahe's observations of the great comet of 1577. He concluded from parallax motions that comets move outside the Earth's atmosphere.

The appearance of the great comet in 1680–1681 was used by Isaac Newton to verify Kepler's laws. This work was not published, however, until 1687 as a result of Edmund Halley's curiosity about the motion of the comets of 1531, 1607 and 1681. This was the first proof that comets orbited the Sun on elliptical orbits.

Up until the advent of spectroscopy in the mid-1800s there was considerable speculation about the nature of comets and whether they shone by reflected sunlight or intrinsic light. By the early 1900s, it was believed that comets must be composed of a mixture of solid and gaseous material and that the material in the tails escaped forever. This led to the belief that comets should wear out quickly [4].

Spectra of a couple of dozen comets from 1868 to 1881 showed bands of lines attributed to 'olefiant gas' (burning oil or hydrocarbons) and the Swan bands of carbon (C_2). The appearance of two great comets in 1882 allowed the first photographic spectra of comets and these showed unmistakeable lines of sodium and bands in the blue that would later turn out to be cyanogen (CN). Improvement in photographic plate sensitivity allowed the detection of cyanogen in comets in the late 1800s, bringing with it speculation as to whether all comets had similar characteristics, or if the gas was acquired as they moved through space. As noted by George Chambers in 1909 when answering the question about the composition of comets, he said '. . .probably the heads are a mixture of solid and gaseous matter, and that the tails are gaseous, the gaseous matter in the tails being the result of the volatilisation of the solid matter of the heads . . .' [4].

In the 1950s, there was an intense debate over the physical nature of comets that was not resolved until the 1986 *Giotto* mission flyby of the nucleus of comet Halley. Dissatisfied with the generally held belief that a theory of planet formation did not need to also take account of the origin of comets because of their vastly different nature, Ray Lyttleton published a paper discussing the origin of comets in 1948. He argued that comets were the result of the coalescence of dust streams gravitationally captured by the Sun as it travelled through interstellar dust

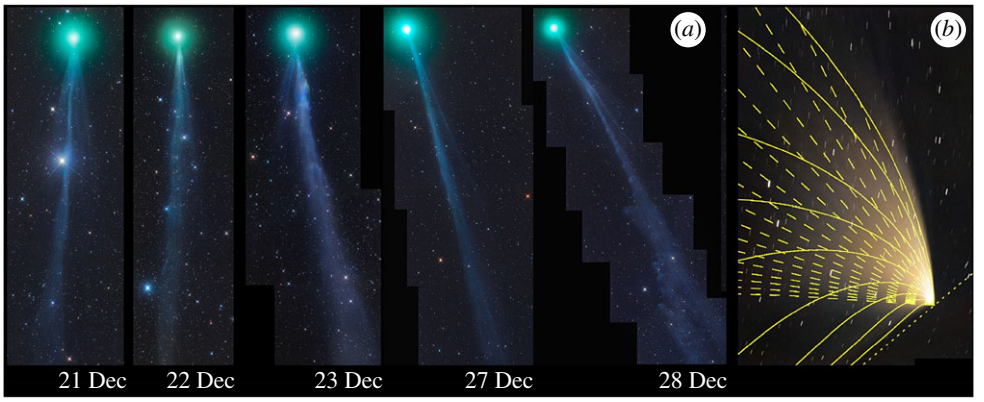

Figure 2. (*a*) Ion tail of comet C/2014 Q2 Lovejoy seen on five dates in 2014 when the comet was at 1.4 AU from the Sun about one month before its perihelion. The images show the changes in the tail over a period of a few days. Images by Gerald Rhemann (www.astrostudio.at) used with permission. (*b*) Broad dust tail of comet C/2011 L4 PANSTARRS obtained by Lorenzo Comolli on 21 March 2013 when the comet was 0.45 AU from the Sun and 1.19 AU from the Earth. Superimposed on the comet are synchrones (dashed) which trace a range of grain sizes released from the nucleus at the same time and syndynes which trace the location of dust grains of the same size released over a range of times. The model is from M. Fulle (INAF/Univ. of Trieste). Used with permission.

clouds [5]. This 'sandbank' theory was in contrast with a second explanation presented by Fred Whipple in 1950 which visualized comets as solid conglomerates of ices mixed with dust. Whipple postulated that sublimating ices came from beneath a dust layer after experiencing a thermal lag. On a rotating nucleus this outgassing delay would result in non-gravitational accelerations that could delay or accelerate the comet's perihelion arrival [6]. This 'dirty snowball' model was used to explain the orbit of comet 2P/Encke. Although most of the scientific community favoured the dirty snowball model, the debate was not settled until 1986 when the European Space Agency (ESA) *Giotto* spacecraft flew past the nucleus of comet 1P/Halley establishing that it had a solid nucleus.

A second remarkable insight into the understanding of comets was made in the 1950s with Jan Oort's deduction of the existence of a vast cloud of comets surrounding the solar system [7]. Using the orbits of 19 long-period (LP) comets corrected for perturbations by the giant planets, Oort showed that there was an excess of comets with semi-major axes between 50 000 and 150 000 AU. He inferred that this required a source population of about 10^{11} comets (0.1–0.01 Earth masses) that were isotropically distributed around the Sun. Stars passing close to the solar system perturb these comets onto orbits bringing them into the inner solar system on LP comet orbits. From the narrow width of the 'Oort spike' in the comet histogram Oort noted that there was a dearth of comets coming into the inner solar system on their second and subsequent perihelion passages. To explain this, he proposed that while stored for 4.5 Gyr in the Oort Cloud, interaction between cosmic rays and volatiles in the comet's surface layers created a 'volatile frosting' of reactive species that disappeared upon heating during the first inner solar system perihelion passage.

The 1950s and 1960s also saw the development of an understanding of the mechanics of comet gas and dust tails. Photographs of bright comets beginning in the early 1900s showed fine structure in tails that changed on short time scales. This was due primarily to emissions from CO^+, whereas the diffuse structure was light reflected from an agglomeration of dust grains. The explanation for the structure of the ion tails was proposed by Biermann in 1951 when he deduced the existence of a flow of particles (solar wind) from the Sun [8]. However, his theory required unreasonably high solar wind densities (10^3 cm^{-3}) and velocities (10^3 km s^{-1}). Alfven [9] avoided this by suggesting that the solar wind carried a frozen-in magnetic field that was forced to drape around the comet by the cometary ions, forming the tail (figure 2*a*). Large accelerations seen in the tail were then due to magnetohydrodynamic waves [10].

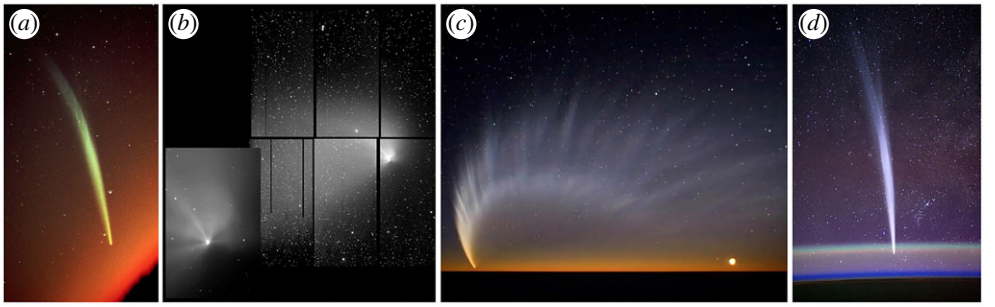

Figure 3. Images of some modern very bright comets. (*a*) C/1965 S1 (Ikeya-Seki), peak mag = −10, photographed from Kitt Peak on 29 October 1965 by Roger Lynds (National Optical Astronomy Observatory/Association of Universities for Research in Astronomy/National Science Foundation). (*b*) C/1995 O1 (Hale-Bopp), peak mag = −1, obtained with the Canada France Hawaii Telescope and the 8K CCD mosaic on 16 September 1996 when it was at 3.1 AU, about 200 days before perihelion, by K. Meech, O. Hainaut and J. Bauer. (*c*) C/2006 P1 (McNaught), peak mag = −6, viewed from the ESO Paranal observatory in January 2007 by Sebastian Deiries (ESO). (*d*) C/2011 W3 (Lovejoy), peak mag = −4, photographed from the International Space Station by NASA astronaut D. Burbank on 22 December 2011 (credit: NASA/Dan Burbank).

Observations of the dust tail of comet 1P/Halley in 1895 led F. W. Bessel to develop a theory of dust tail structure that relied on a combination of a repulsive force and solar gravity. This was subsequently expanded upon by F. A. Bredichin who introduced the concept of syndynes and synchrones (an example is shown in figure 2*b*) which mapped out the location of particles of a range of sizes released at a range of times. Solar radiation pressure was suggested as a candidate for this force in 1900 by the Swedish chemist S. Arrhenius. In 1968, Finson and Probstein developed a realistic three-dimensional dust-dynamical model. Information about activity levels, grain sizes and ejection velocities can be inferred by evaluating their trajectories under the influence of solar gravity and radiation pressure [11].

Thanks to a modern supply of 'great comets' (figure 3) and the development of new instrumentation for large telescopes, combined with a legacy of several decades of dedicated surveys to characterize the orbits, chemistry and physical properties of comets, we now have a picture of comets that is quite different from the initial models developed in the 1950s. Today there are three cometary reservoirs: the Oort Cloud, the Kuiper Belt and scattered disc and the main asteroid belt. Comet classes are distinguished by their orbits. The Tisserand parameter, T_J, is calculated from orbital elements and is a proxy for the dynamic orbital class where $T_J > 3$ for asteroids, $2 < T_J < 3$ for short-period comets, $T_J < 2$ for long-period comets. The specific comet classes discussed here include:

— Long period (LP): orbital periods greater than 200 years.
— Dynamically new (DN): a LP comet determined to be making its first pass through the inner solar system from the Oort Cloud. A LP comet is considered dynamically young if it has likely made only a few inner solar system perihelion passages.
— Short period (SP): orbital periods less than 200 years.
— Jupiter family (JF): SP comets whose orbits are controlled by Jupiter and which have periods less than 20 years with low inclination orbits.
— Halley type (HT): comets of intermediate period (between 20 and 200 years) which have high inclination. Their source region is likely the Oort Cloud.
— Encke type (ET): any SP comet whose orbit is inside of that of Jupiter's orbit.
— Main belt comet (MBC): these objects are dynamically asteroidal with $T_J < 3$, but with dust tails that are believed to be driven by volatile sublimation.

Our definition of what distinguishes a comet from an asteroid is blurring, with a continuum of small body compositions between volatile rich and volatile poor.

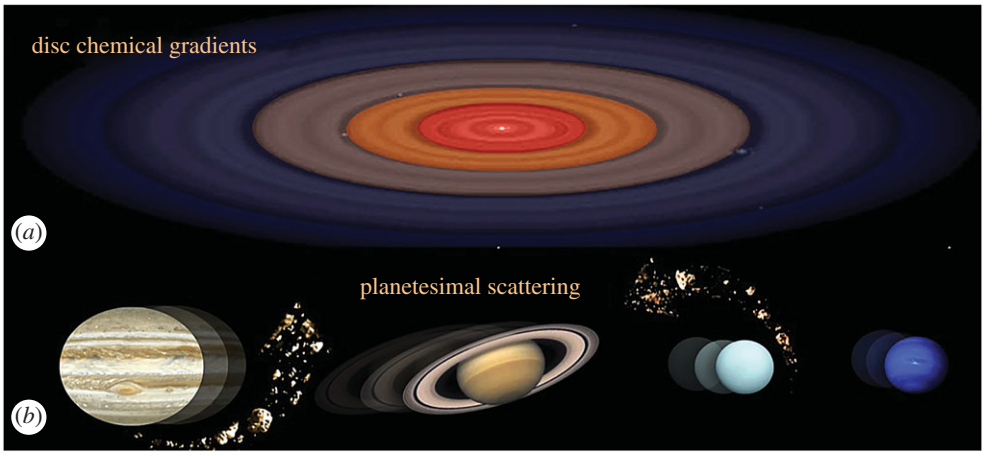

Figure 4. (*a*) Gas leaves a chemical signature imprinted on dust in the protoplanetary disc as it freezes, and this material is incorporated into planetesimals. (*b*) This material may be subsequently scattered as the giant planets grow and migrate. Understanding what comets tell us about the early solar system requires knowledge of chemistry and dynamics.

2. Comet formation

Small primitive bodies were witness to the solar system's formative processes. When gas was present in the disc, during the first few million years of the solar system formation, a local chemical signature was imprinted on the planetesimals (figure 4*a*). Ices condensed out of the nebular gases far from the Sun, outside their respective 'snowlines', and this dictated the different chemistry of the terrestrial and gas giant planets. The connection to today's solar system relies on how this material was dynamically redistributed during planet formation (figure 4*b*).

The classic picture of a protoplanetary disc with a uniform radial heliocentric temperature dependence has radically changed because of advances in modelling and observation. Today's disc models employ chemical networks with hundreds of gas phase and grain species reactions, coupled with hydrodynamic models which are functions of star and disc mass and mass accretion rates, and which take account of angular momentum transport, turbulence and magnetic fields. The resulting chemical maps show complex molecular distributions both radially and vertically.

In the classical dynamical planet formation model, the protoplanetary nebula collapsed to a flattened disc and planetesimals began to grow, hierarchically sticking together through electrostatic forces. The planetesimals grew larger and larger until runaway growth occurred and the gas giant cores were large enough to capture nebular gas [12,13]. The terrestrial planets grew from planetesimals and planetary embryos from the inner disc with a surface density varying smoothly as a function of distance from the Sun [14,15]. Comets were icy planetesimals left over after planetary growth. The old paradigm was that comets that formed in the vicinity of the gas giants were scattered outwards to populate the Oort Cloud. Today these are scattered inward to become the LP comets. Planetesimals forming beyond the giant planet region, at lower temperatures in the Kuiper Belt, remained there until scattered inward to become Centaurs and eventually SP comets [16]. This scenario of the two reservoirs forming at different temperatures implies that they should today have different chemistries.

The dynamical landscape has been rapidly evolving. There are now several dynamical models that can reproduce much of our solar system's current architecture. These fall into three major categories: (i) growth in a gas and dust disc with large-scale planet migration, (ii) growth in a disc with an uneven mass distribution, and (iii) rapid growth from centimetre-scale pebbles to planetary embryo size. However, some key details of our solar system (and others) are not well explained in all the models, e.g. overcoming the metre-sized growth barrier, the small size of Mars, and the architecture seen in many exoplanetary systems.

The 'Grand Tack' model [17] starts the solar system formation simulation at an early phase when the giant planets grew and migrated in a gas-rich protoplanetary disc. During their inward migration, the giant planets scattered inner solar system material outward, their inward migration halted due to a resonance between Jupiter and Saturn. As the planets migrated outward, they implanted a significant amount of icy planetesimals from 3.5 to 13 AU into the inner solar system and populated the outer solar system with rocky and icy material. After dispersal of the gas disc within the first 10 Myr, the giant planets interacted with the massive disc of planetesimals beyond the orbits of the giant planets, dispersing the planetesimals (the 'Nice' model [18]). About 5% of this material ended up in the Oort Cloud and 1% in the scattered disc. In the 'Depleted Disc' model [19] the terrestrial planets grow (after Jupiter and Saturn are fully formed) from a disc of planetesimals and embryos that do not follow a uniform distribution as a function of heliocentric distance. The non-uniformities prevent Mars from growing too large. In the third approach, the 'Pebble Accretion' model [20], planetary embryos are grown efficiently when pebbles are slowed by gas drag. A few assumptions were made on the protoplanetary disc structure which favoured a mass distribution strongly concentrated within 1 AU, resulting in a small Mars and one planet the mass of the Earth. In this model, there is no giant planet migration.

The classical comet formation scenario implies there should be chemical differences for comets that originated in today's different dynamical reservoirs and significant effort has gone into searching for these differences. Interpreting what comets tell us thus requires understanding the connections to the chemistry of the protoplanetary disc, and to the dynamical evolution of the planetesimals. The modern models make very different predictions about planetesimal scattering in the early solar system. These can be observationally tested.

3. Cometary volatiles and their release from the nucleus

After the initial suggestions of highly reactive radicals on the surface of first passage (e.g. dynamically new) LP comets by Oort [7], many researchers have tried to understand the source of the different species seen in cometary comae. Wurm [21] suggested that these were fragments photodissociated from parent molecules that directly sublimated from the nucleus. By contrast, pioneering work by Delsemme and Swings suggested that the appearance of different species seen in the comae of comets was controlled by water, and that they were stored in solid hydrates (clathrates) [22]. Cowan and A'Hearn were the first to apply a water and CO_2-ice vaporization model employing the energy balance at the surface to explain the brightness behaviour of cometary nuclei as a function of heliocentric distance [23]. This technique was used by Meech *et al.* [24] to explain the appearance of activity for Halley's comet in 1985.

These simple surface sublimation models were sufficient to show that activity in SP comets (inside approx. 6 AU) was largely controlled by water-ice sublimation, but that LP comets active at larger distances was controlled by volatiles with lower sublimation temperatures. From protoplanetary disc chemistry, the next most abundant species suggested that this was likely due to CO or CO_2-ice sublimation [25] (figure 5*a*).

This 'standard model' of activity, however, did not take into account diurnal surface temperature variations, heat conduction into the interior (both in the surface layers and at depth), the development of an insulating dust mantle or the effect of porosity on gas flow through a porous medium. Modern state-of-the-art three-dimensional thermal models take account of all of these factors, as informed by laboratory experiments of cometary simulants [27]. These models assume that the comet nucleus is a very porous mixture of dust and ice grains, where the dominant volatile is water ice. Other species are present as solid ices mixed in, or are trapped in amorphous water ice or water ice clathrates [28]. As solar heat penetrates into the comet the models show that there will be a structural evolution of the surface layers (figure 5*b*). As the comet evolves thermally, the thermophysical properties of the upper layers also change.

This type of model was used to successfully explain the near-simultaneous appearance of species of widely differing volatility in comet C/1995 O1 (Hale-Bopp) [26,29], the outburst in comet 1P/Halley and activity in 95P/Chiron, among others.

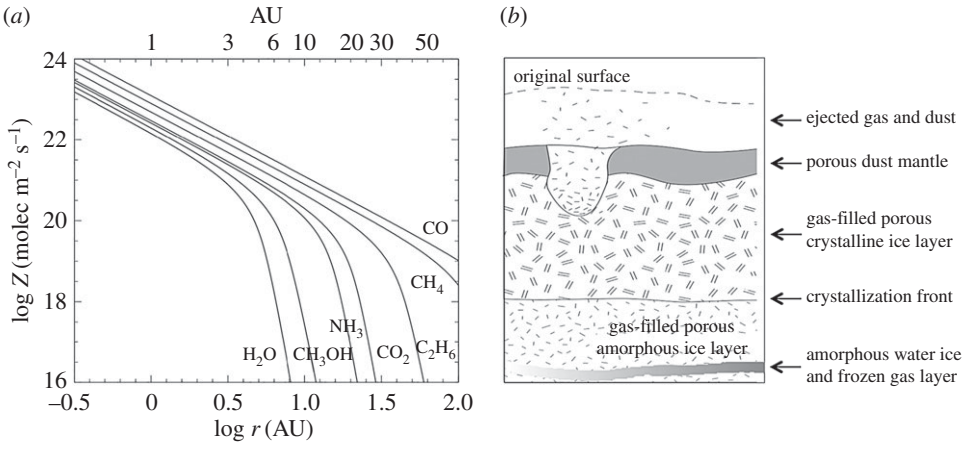

Figure 5. (*a*) Molecular production rates for pure ices as a function of heliocentric distance for an isothermal nucleus of 4% albedo. Contrary to the commonly held misconception that comets 'turn on' at the point where these vaporization curves have their inflection points (3 AU for water ice), comet activity can be quite strong at this point. The flux of sublimating water molecules is strong enough between 5 and 6 AU to lift optically visible dust (0.5 μm grains) off the nucleus [25]. (*b*) Schematic layered structure of the nucleus of a comet (after [26]).

4. Volatiles: pristine from the interstellar medium or processed material?

One of the goals of assessing the comet volatile inventory has been to understand to what extent material in comets has been processed during formation or if it represents pristine material inherited from the interstellar medium (ISM) [30].

At optical wavelengths, two long-term surveys of cometary spectra [31,32] showed that there were chemical differences seen among comets in terms of their 'daughter' species (the photodissociation products from the parent molecules sublimated directly from the nucleus). These surveys showed that the relative abundance of C-chain species fell into two classes: normal and depleted. As shown in figure 6*a*, which plots the abundance of C_2 relative to CN as a function of Tisserand invariant, nearly half of the SP JF comets were depleted, whereas very few of the LP comets were. A'Hearn suggested that there were some places of comet formation that were compositionally distinct, attributing the depletion to some sort of thermal process [31].

Information on the parent volatile species has come through observations at radio and near-infrared wavelengths. As in the case of the daughter species, strong diversity has been seen in comet parent molecules—both among comets, and in individual comets as a function of rotation or observations taken at different times. The abundance of CO, CO_2, hydrocarbons and other species varies by at least a factor of 10 (and higher for CO) [30,33]. The number of comets for which these measurements has been made is still too small to see clear correlations in chemistry between dynamical classes. However, as seen at optical wavelengths there is an emerging trend showing that there are comets normal, enriched and depleted in the hydrocarbon species [33,34]. Members of the different dynamical classes are found in each group.

This chemical diversity in comets with representatives across all dynamical classes may be a signature of dynamical movement of material in the protoplanetary disc.

5. Insights from missions and space observatories 1986–2011

Our view of the comet nucleus has evolved from the original concept of Whipple's 'dirty snowball' to a collisionally modified (but possibly largely primordial) porous rubble pile of low density and low strength [35]. A collisionally evolved population is predicted by the Nice dynamical model [17]. Data from space missions have shown that each nucleus is unique

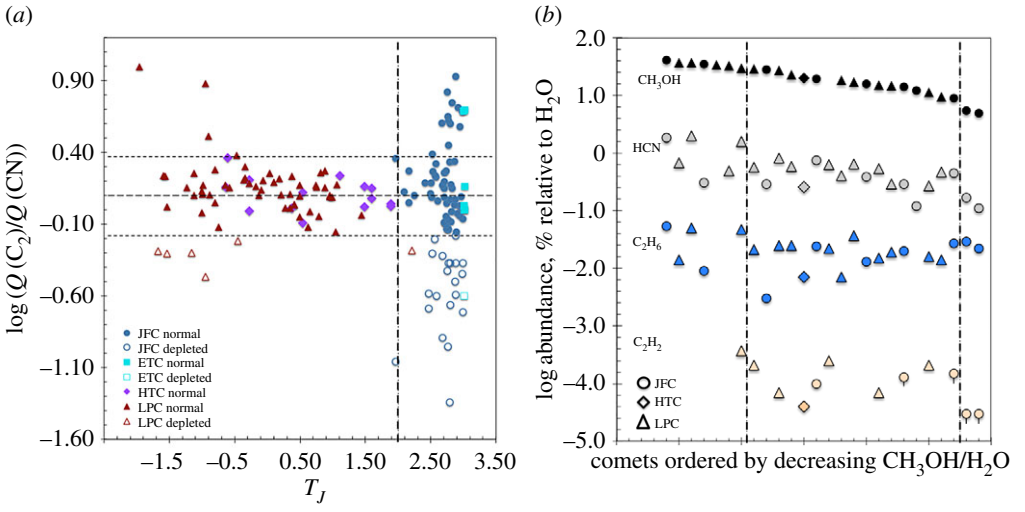

Figure 6. Chemistry of C-chain species and volatile organics plotted versus Tisserand invariant as a proxy for dynamical class. (*a*) Ratio of C_2 to CN abundance as obtained from [31,32], showing that the strong C-chain depletion is found primarily in JF comets. The dashed horizontal lines show the boundaries between normal, depleted and enhanced species [31]. (*b*) Abundances of volatile organic species obtained by several groups as summarized in [33,34]. As in the case of the C-chain compounds, some comets are enriched, normal and depleted (delineated by the vertical lines, after [33]) in parent organic volatile species.

(figure 7). The *Giotto* flyby of comet 1P/Halley showed an irregular surface, with rounded pits, hints of albedo differences and activity originating from discrete areas (bright jets).

The *Deep Space 1* flyby of the nucleus of 19P/Borrelly in 2001 was the first close-up view of a comet's surface sufficiently unobscured to obtain photometric properties and a detailed view of the morphological features. The nucleus showed a bilobate structure, with distinct morphological terrains including mesas, smooth regions, troughs and pits [36]. As in the case of comet 1P/Halley, activity emanated from jets, here concentrated near the smooth regions.

The flyby of comet 81P/Wild 2 provided even higher resolution (22 m pixel^{-1}) and showed a rounded nucleus with morphology dominated by pits and large flat-floored depressions. While ground-based observations of split comets, and the tidal splitting of comet D/1993 F2 (Shoemaker-Levy 9) suggested that comet materials had very low strength, some of the features on 81P/Wild 2 showed overhangs that required some surface material strength.

With each new mission and increase in resolution, complex details on the surface are revealed, and with the *Deep Impact* and *Stardust-NeXT* missions where resolution enabled features as small as a few metres to be seen, it was possible to start to make geological maps and examine geological processes. *Deep Impact* revealed a variety of terrains on the nucleus of comet 9P/Tempel 1, but the new feature that dominated the surface was extensive layering [37]. These ranged from thin metre-scale layers to layers tens of metres in thickness extending up to a kilometre in length. These layers prompted a new model of comet formation called the 'talps' model [38], suggesting that they grew from very low velocity collisions between highly porous bodies which resulted in the disaggregation of one of the bodies spread out as a layer. Talps is an anagram for splat.

Three smooth flow regions were seen on the surface of 9P/Tempel 1, tens of metres thick, and these bear a strong resemblance to the smooth features seen on comet 19P/Borrelly. In the time between the *Deep Impact* and *Stardust-NeXT* missions in 2005 and 2011, there was evidence for the edge of the flows having receded in places by more than 10 m. This, and the suggestion that some jets may have originated from the flow fronts, indicated that these layers may have been volatile rich. The mechanism for the emplacement of the flows has been suggested to be cryovolcanism [39,40]. Analysis of the thermal properties of the surface indicated that the thermal

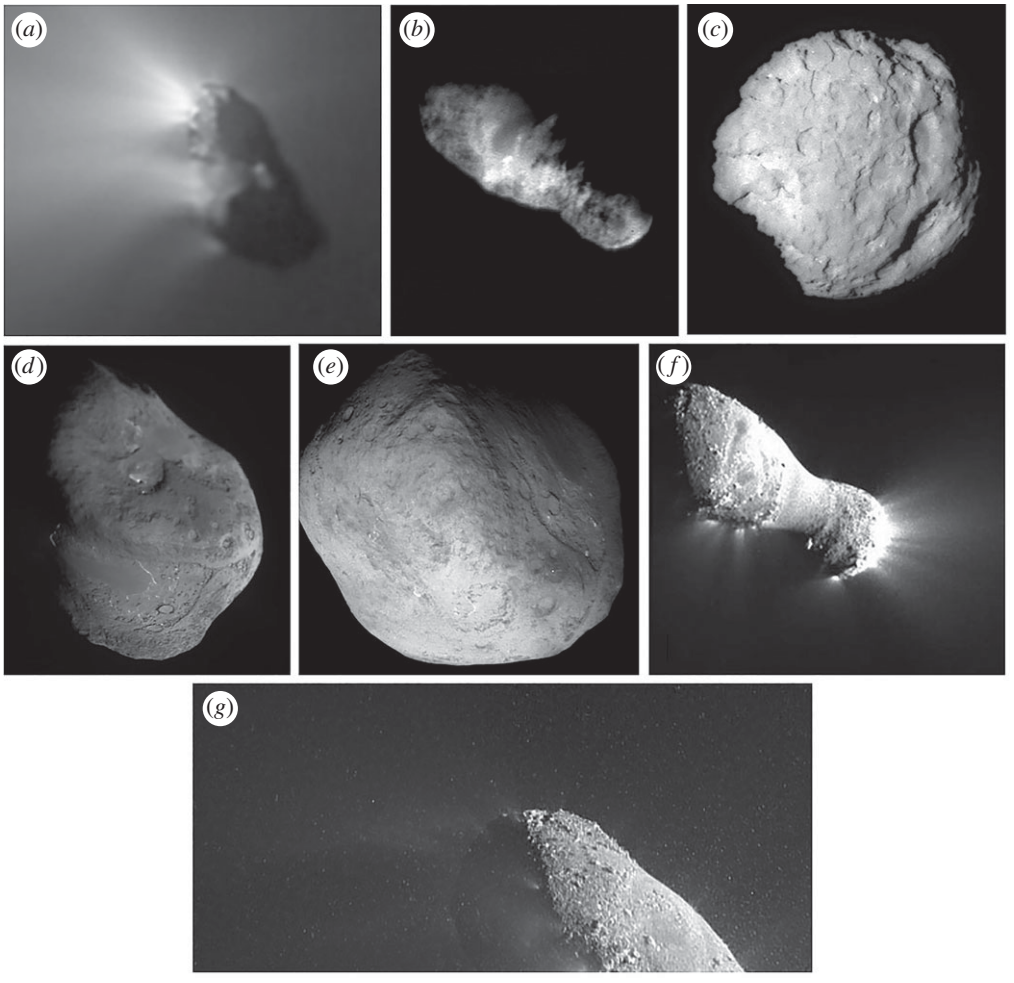

Figure 7. Montage of comet nuclei as visited by spacecraft from 1986 to 2011. (*a*) Nucleus of comet 1P/Halley (15.3 × 7.2 × 7.2 km) as obtained by the Halley Multicolor Camera Team (*Giotto*, MPAe, ESA) as it flew through the coma on 12 March 1986 from a distance of 1372 km. (*b*) Comet 19P/Borrelly (8.0 × 3.2 km) as seen at a distance of 3556 km by the *Deep Space 1* mission. Resolution: 47 m pix^{-1}. Credit: NASA/JPL. (*c*) Comet 81P/Wild 2 (5 km in diameter) viewed at the time of closest approach (238 km) on 2 January 2004 by the *Stardust* spacecraft. Credit: NASA/JPL. (*d*) Nucleus of comet 9P/Tempel 1 as seen from the *Deep Impact* mission on 4 July 2005 from a distance of 500 km. The 5 km long nucleus shows layering, and rounded pits as well as smooth terrain. Credit: University of Maryland, JPL/NASA. (*e*) A view of the back side of the nucleus of comet 9P/Tempel 1 as seen during the *Stardust-NeXT* flyby on 14 February 2011 from a distance of 181 km. (*f*) Comet 103P/Hartley 2 at close approach during the *EPOXI* mission on 4 November 2010 from a distance of 694 km. The nucleus maximum length is 2.33 km. Credit: NASA/ JPL-Caltech/UMD. (*g*) Close-up of comet 103P/Hartley 2 from the *EPOXI* mission showing the night-side jet activity, and the swarm of large near-nucleus particles.

inertia of the surface layers was of the order of 10 times lower than previously suggested, hinting that comets might preserve pristine material close to the surface.

The *Stardust-NeXT* mission flyby of comet 103P/Hartley 2 showed another bilobate nucleus similar in shape to comet 19P/Borrelly (figure 7*b*,*f*). Two types of terrain were seen on the surface: smooth regions seen in the waist region between the two lobes, and on parts of the larger lobe, and knobby terrain. Active jets were seen everywhere, but were clustered in the knobby terrain at the end of the smaller lobe (figure 7*f*). The pits seen on 81P/Wild 2 and 9P/Tempel 1 were not seen on this comet, and the smooth terrains do not look like the flow regions on either 19P/Borrelly or 9P/Tempel 1, and there is no thick large-scale layering on this nucleus as seen on 9P/Tempel 1.

However, while 103P/Hartley 2 is the smallest of the nuclei visited by spacecraft, it was by far the most active, even considering the heliocentric distance. Unlike the other comets 103P/Hartley 2 was surrounded by large aggregates of material, likely lifted off the nucleus from the numerous jets, many of which emanated from night-time side (figure 7*g*).

The nucleus densities measured *in situ* and estimates from the ground suggest that JF comets are low strength and probably all have bulk densities $<0.5\,\mathrm{g\,cm^{-3}}$. For bodies that are a mixture of ice and rock this implies very high porosity >70% [37].

(a) CO_2 as a driver of activity

One of the new insights to come from the *Deep Impact* flyby of 9P/Tempel 1 was the indication that CO_2 and H_2O had very different distributions around the nucleus, suggesting that the nucleus was made of cometesimals of different chemical compositions. More strikingly, from both ground-based observations of comet 103P/Hartley 2 and the *in situ* data, it was clear that at perihelion, CO_2 was the main driver of activity [41].

Because the Earth's atmosphere is opaque at the wavelength at which CO_2 radiates, direct measurement of this molecule requires space observations. The *Spitzer*, *Akari* and *WISE* space satellites have recently provided significant information about the abundance of CO_2 in comets. However, even before direct measurements from space there were hints that CO_2 played an important role as a driver of activity. Estimates of water production rate measured in the ground-based spectra surveys [31,32] coupled with estimates of nucleus size showed that most comets were active over a very small fraction of their surfaces (a few per cent).

However, there was a long tail on this distribution, with some comets, such as 103P/Hartley 2, showing fractional active surface areas > 100%. This appears to be an indication of a second source for water sublimation, e.g. the large agglomerates seen in the coma with the *in situ* observations of 103P/Hartley 2. Ice-sublimation models [42] for this comet show that the pre-perihelion behaviour was well fitted with water ice driven activity until within two months of perihelion, then CO_2 activity dominated (figure 8*a*). While this is an approximate ice-sublimation model which assumes a dust/gas ratio of one [24], it has been very successful at interpreting the basic activity behaviour for comets, including predicting the water production rate for comet 67P/Churyumov-Gerasimenko at the time Rosetta instruments first detected water [44]. This was also the time that the nucleus spin rate started to change dramatically [45]. Laboratory experiments on thick ice samples showed that sublimation from deeper volatile layers could result in the ejection of large chunks of material [46,47]. Modelling the brightness data for other comets, both LP (figure 8*b*) and SP comets, shows the importance of CO_2 for controlling activity, and is a good proxy when *in situ* observations are not available.

Data on comet CO_2 abundances from infrared space satellites are shown in figure 9. The abundance of CO_2 varies significantly between both LP and SP comets, ranging from a few to 30% as measured inside approximately 3 AU where water is strongly sublimating. There is no significant difference between LP and SP comets in the range of CO_2 production. As in the case of other chemical markers, there is a suggestion that there are some comets strongly depleted in CO_2. From this it is likely that the LP and SP comets formed in overlapping regions [51].

When one examines the radial and vertical maps of molecular abundances coming from state-of-the-art disc chemistry models, it is clear there is likely complex variation in the ratio of volatile species expected in the comet forming regions [52]. Once possible planetesimal movement is considered from dynamical scattering, it is perhaps unsurprising that there is a range in volatile abundances and that it is not strongly correlated with dynamical class.

(b) Nucleus size and surface properties

Nucleus size is a fundamental property that has important implications for constraining solar system formation models. From two large space near-IR surveys (SEPPCoN [53] and NEOWISE [50]) nuclei are seen to be relatively small, with a median radius of approximately 1.4 km

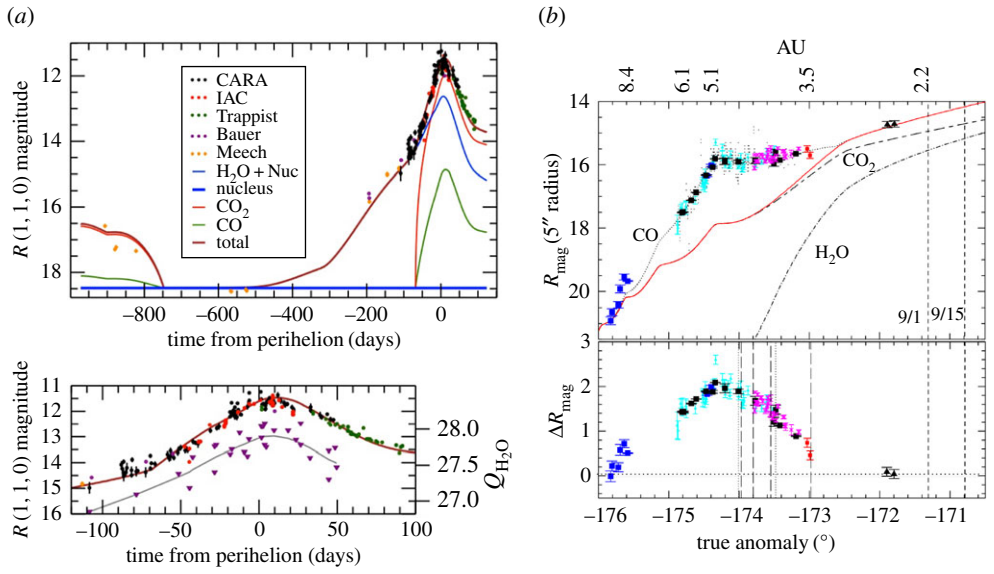

Figure 8. (*a*) Absolute brightness for comet 103P/Hartley 2 (shown as points). The data were well fitted with the standard water ice sublimation model until about two months before perihelion when activity driven by CO_2 began to dominate [42]. The bottom panel expands the data around perihelion and shows the agreement with measured ground-based water production rates (purple triangles; lower curve). (*b*) Apparent photometric light curve for comet C/2012 S1 (ISON) fitted with the standard ice sublimation model showing that the activity at large heliocentric distances was controlled by CO_2 (red curve) with an outburst due to CO [43]. The CO outburst creates the excess brightness seen between true anomalies −176° and −173°. The bottom panel shows the difference between the total light curve and the CO_2 plus H_2O models.

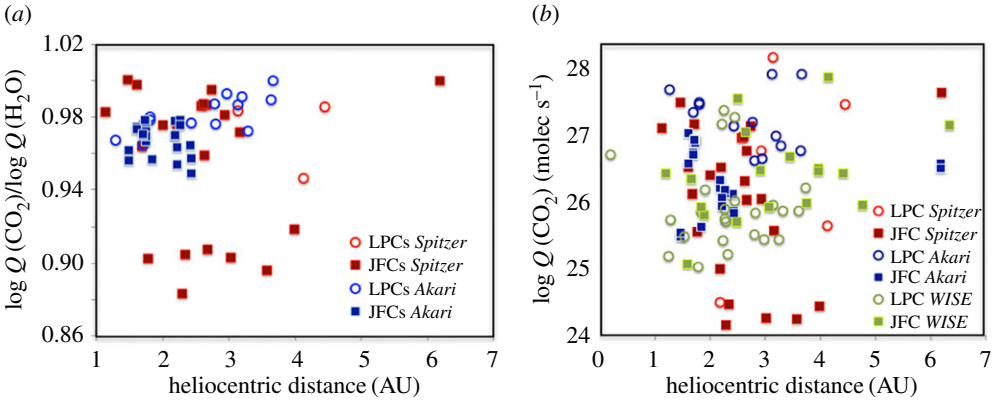

Figure 9. (*a*) CO_2 abundance relative to water as a function of dynamical class from two near-IR space surveys [48,49]. There is no strong trend in CO_2 abundance with distance. (*b*) CO_2 production rate as a function of distance showing the *WISE* measurements for which there is no simultaneous measurement of the water production [50].

(figure 10), and a cumulative size distribution with a power law slope of −1.9, consistent with a collisional population but truncated at sub-kilometre sizes. There are many fewer reliable nucleus size estimates of LP comets compared to the SP JF comets; however, a Student's *t*-test shows that at present there does not appear to be any size difference between the populations.

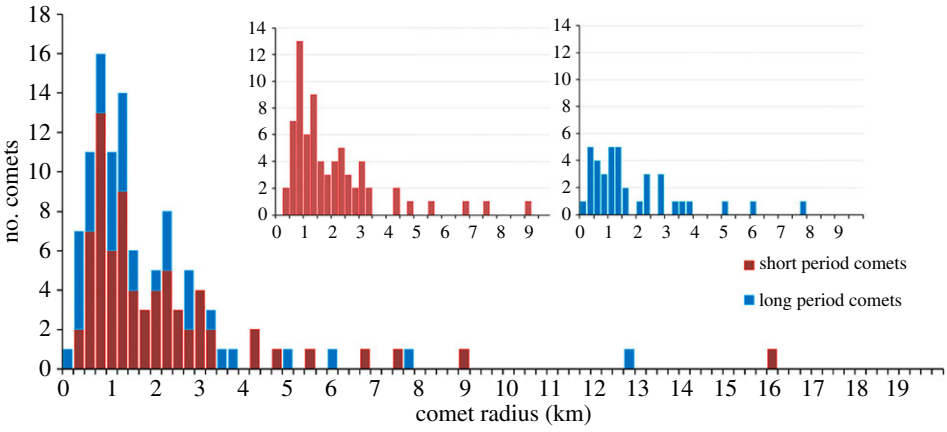

Figure 10. Comet nucleus size distributions measured in the near-IR from space [50,53]. The insets show the histograms for the distributions of LP and SP comets separately. The median radius for the SP comets is 1.46 km and for the LP comets 1.3 km with a Student's *t*-test probability of 89% that these are drawn from the same population [50]. (Online version in colour.)

Analyses of the photometric properties of four nuclei visited by spacecraft show that the nuclei are uniformly low albedo with global averages near 4%, consistent with what had been inferred from ground-based observations. Variations of approximately 10% are seen across the surfaces, with some localized areas as much as twice as bright [54]. This is consistent with limited areas of water–ice frost (containing a few per cent water) intimately mixed with the surface materials on the dawn terminators [55]. The colours of comet nuclei have been known to be moderately red from the ground [56], and this was also seen with the *in situ* observations. However, colour variations were seen across the nucleus, possibly due to the existence of icy patches. Nucleus phase functions are similar to those of C-type asteroids, with phase slopes of $\sim 0.05\,\mathrm{mag\,deg^{-1}}$ [57].

(c) Isotopes

The deuterium to hydrogen (D/H) ratio has long been held up as the key fingerprint for tracing the origin of volatiles in the solar system. At low temperatures (less than 30 K) ion–molecule reactions enrich the D/H ratio over its starting values. In the protoplanetary nebula D/H evolved from an initial supply of highly enriched water from the ISM via active chemistry at cold (less than 30 K) disc temperatures that also increased D/H. Mixing with hot inner nebula equilibrated gas led to sharp gradients in the disc. It was long thought that relating the D/H values for different reservoirs of objects would lead to an inference about the temperature and hence radial location in the disc from which the volatiles originated. When the first D/H measurements for LP comets were found to all be about twice that in the Earth's ocean water (figure 11*a*), this was believed to be evidence that comets contributed to the D/H enrichment seen in Earth's oceans [60]. When D/H in the first SP comet was measured, for comet 103P/Hartley 2, it was expected that the D/H would be higher than that of the LP comets based on disc chemistry models. When it turned out that the value was the same as ocean water [61] this spurred revision of disc chemistry models.

The oxygen isotopic makeup (^{16}O, ^{17}O and ^{18}O) of the original oxygen-bearing compounds in the protoplanetary disc is determined by a process called 'self-shielding'. This is the consequence of solar UV selectively photodissociating different CO isotopologues in the disc at different distances, allowing oxygen to combine with hydrogen, making water. On a three-isotope diagram (figure 11*b*), all terrestrial samples plot along the terrestrial fractional line, whereas primitive chondrites plot along a mass-independent fractionation line (CCAM) [62]. It is inferred that this line results from mixing of two isotopically distinct reservoirs, one ^{16}O-rich and one ^{17,18}O-rich,

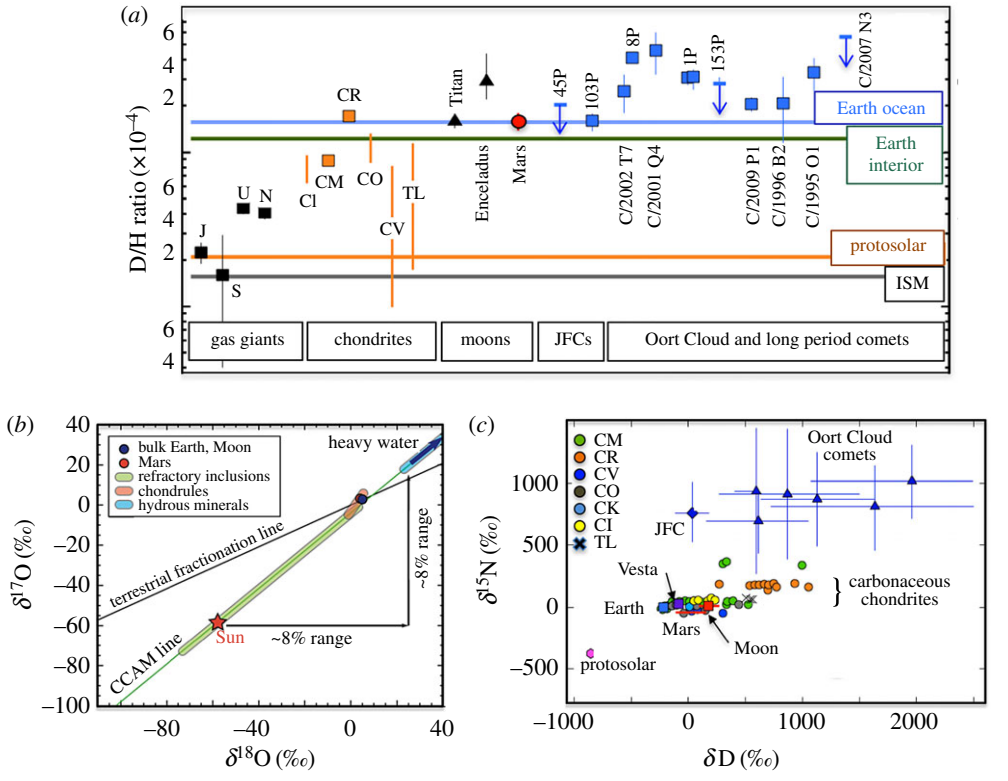

Figure 11. (*a*) Summary of D/H reservoirs in the solar system prior to the Rosetta mission. (*b*) Oxygen three-isotope plot showing major solar system reservoirs. Figure after [58]. (*c*) Variation of D/H and nitrogen isotopes in solar system reservoirs. Figure after [59].

the latter thought to be the result of CO self-shielding [63]. The total range in oxygen isotope variation seen in the solar system is only 8%. This ratio has been measured only in a few comets with uncertainties around 10% [33]. However, distinguishing different reservoirs and formation distances will require measurement precisions of 1% for oxygen in water and 3% in CO (to account for all the oxygen), thus more measurements are needed.

The solar nebula and Sun are depleted in ^{15}N relative to the Earth's atmosphere, whereas other reservoirs are enriched [64]. The cause of this large fractionation is not well understood. It may be inherited from the protosolar cloud, or it can be the result of photochemical self-shielding effects in the disc. To date there have been a couple dozen nitrogen-isotope ratios measured in comets, all from remote sensing, and these all show an enrichment in ^{15}N [59]. A summary of comet isotopic measurements may be found in [65].

(d) Dust

The *Giotto* mission mass spectrometry of dust from 1P/Halley showed that the dust had elemental abundances typical of rock-forming minerals and that additionally the grains were rich in organics (C, H, O and N).

The chemical conditions in the solar nebula control the chemistry of the silicates that are seen in comets. In contrast with the ISM where Fe–Mg amorphous silicates are abundant, ground-based observations of comets show that Mg-rich crystalline silicates dominate [66]. This is an indication that they formed in the hot inner disc and is evidence of radial transport of material. The lack of aqueous alteration products seen in the dust compared to asteroidal material indicates that

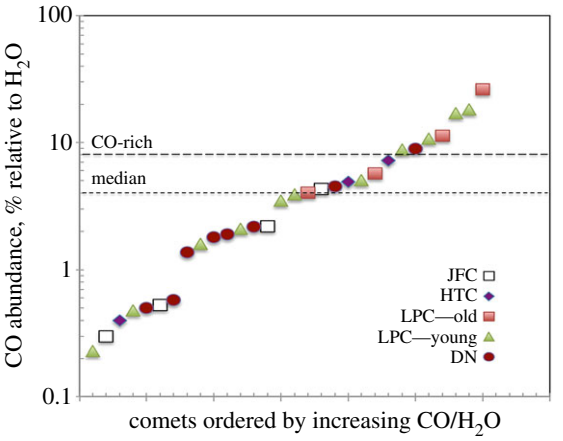

Figure 12. CO abundance in comets of different dynamical classes ordered by increasing CO/H_2O ratio. Dynamically new (DN) comets are those that are making their first passage through the inner solar system from the Oort Cloud. Figure after [71] including data from [34,71,72]. The boundary between CO-rich and CO-normal comets is arbitrarily defined as twice the median value, following [71]. (Online version in colour.)

refractory material in comets likely accreted prior to asteroid parent bodies, and may reflect a combination of ISM material and processed nebular minerals [66].

Samples returned from the *Stardust* mission showed that the refractory material was similar to that of primitive meteorites and condensed at high temperature, with similar isotopic compositions. However, unlike meteorites which show distinct chemical groupings related to their formation regions in the nebula, i.e. local processes, comet dust appears to have sampled a very wide range of formation distances. The dust analysis shows evidence for large-scale mixing in the nebula [67,68].

Spectra taken during the *Deep Impact* event also showed crystalline Mg-silicates indicative of nebular processing, although the spectrum from the *Spitzer* telescope showed possible evidence of hydrated minerals [69].

6. Cometary reservoirs: key questions

The *Deep Impact* and *EPOXI* missions made measurements in the near infrared and found for both 9P/Tempel 1 and 103P/Hartley that the surface materials had very low thermal inertias. Thermal data for 57 comets from the SEPPCoN survey suggested that the surfaces of these comets likely had thermal inertias similar to 9P/Tempel 1 [53]. With the low strength, highly porous surfaces that insulate comet interiors, one of the fundamental new insights from the missions was that pristine material is likely accessible near the surface [70]. This is of key importance for the next generation of comet sample return missions as this will allow the sampling of pristine materials that can help answer questions about origins. While the interiors may be pristine, there are clearly a lot of active surface processes that need to be understood about volatile transport to make these connections—the Rosetta mission is designed to provide this information.

The modern era of exploration both from the ground and space has enabled a new understanding of comets and the information that they provide about the early solar system. We can now use a wealth of chemical and isotopic fingerprints to compare with protosolar disc models. We have seen that CO_2 plays an unexpectedly key role in controlling comet activity in many comets, and that this is not apparently correlated with comet dynamical classes. However, the information from the highly volatile CO is telling us something different. There are now 30 comets for which we have good measurements of CO relative to H_2O (figure 12).

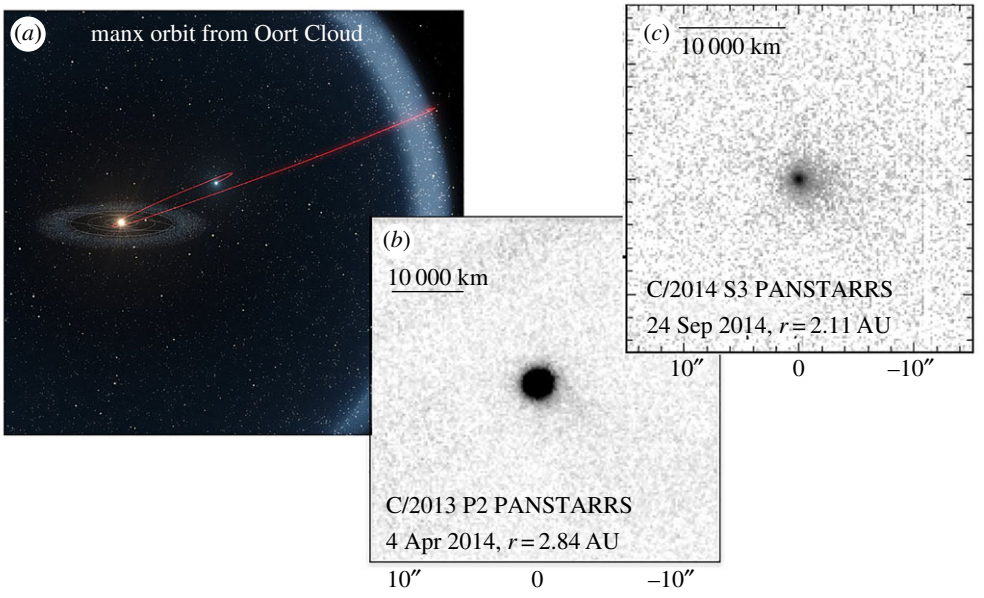

Figure 13. Manx comets may provide key tests of solar system dynamical models. (*a*) Manx comets are perturbed inward from the Oort Cloud on long-period orbits. Credit EOS/L. Calcada. (*b*,*c*) Images of two Manx comets near perihelion showing extremely low-level activity, approximately 10^3 times less active than low-activity JF comets and 10^4–10^6 times less active than typical LP comets at similar distances. (Online version in colour.)

The range of CO abundances varies significantly, ranging from less than 1% to 30% relative to water. Of note is the fact that in the group of CO-rich comets, there are no SP comets—all are LP comets. Figure 12 shows that while the comets with the most CO are LP comets, they are not the ones known to be making their first passage through the inner solar system. This may suggest that this is not an artefact of evolution, rather a native property of these comets; however more data are clearly needed. It should be noted that many of the dynamically new comets on their first passage through the inner solar system are CO-depleted. It is possible, however, that many of the most brilliant historical comets (figure 1) were in fact also CO-rich. This wide distribution of the most volatile cometary molecules within the LP comets argues again for wide scale dynamical mixing in the early solar system—i.e. that the classes we see today are not closely tied to well-defined formation locations.

In recent years, new types of comets have been discovered which are providing clues to early solar system dynamical processes and the distribution of volatiles in the protoplanetary disc. One of these classes is the MBCs. These are objects residing today in the main asteroid belt, dynamically asteroidal, but with clear signatures of activity that is likely driven by water-ice sublimation [73,74]. The first, 133P/Elst-Pizarro, was discovered in 1996, but these were not recognized as a class until 2006 with the discovery of two more [75]. It is likely that many may have formed *in situ*, and that the entire outer asteroid belt is wet, with extant ice existing today. Water was clearly a key ingredient in this region of the early solar system as seen by the extensive aqueous alteration in asteroid parent bodies. MBCs present opportunities to sample the isotopic fingerprints in volatiles in a region of the solar system much closer to the Sun than we have had access to previously.

In 2013, the PanSTARRS telescope in Hawai'i discovered a second potentially new type of comet that may be a key for constraining solar system dynamical models [76]. These are objects on LP comet orbits which exhibit little or no activity near perihelion at distances where water-ice sublimation should be strong. They have been termed 'Manx comets' for their nearly tailless appearance (figure 13).

What makes these objects particularly interesting is that one of them, C/2014 S3, shows a surface mineralogy consistent with rocky inner solar system S-type material [77]. The implication is that this object which formed in the warm inner solar system was ejected outwards into the Oort Cloud and is now making its way back to the inner solar system on a LP comet orbit. The amount of inner solar system material that can get dynamically ejected to the Oort Cloud early in the solar system's history varies dramatically between current dynamical models. A strong test of these models will be to assess the fraction of Manx comets that are rocky.

Additionally surprising is that a rocky S-type body has a tail that is consistent with water outgassing. S-type asteroids are the known parent bodies of the ordinary chondrites and these have seen minor amounts of aqueous alteration. With the S-type Manx comets, we may be looking at fresh inner solar system material that has been preserved for billions of years in the Oort Cloud.

7. Conclusion

A pre-Rosetta exploration of the cometary volatile inventory has shown both enrichments and depletions in parent volatile organics and carbon-chain species which are not correlated with dynamical classes. Isotopic information is known for a subset of these comets. Samples returned from the *Stardust* mission indicated that there was wide-scale migration of disc material and that refractory comet dust experienced high temperatures near the Sun. Both ground- and space-mission data have shown that comets are not chemically homogeneous, although further work is needed to understand whether this is primordial or evolutionary. A key result from space observations has been the realization that CO_2 can be a major driver of activity—both for SP and LP comets. New comet classes, the MBCs and the Manx comets may provide key insights into the early solar system volatile distribution and dynamics.

Understanding the formation location of comets likely needs multiple isotopic measurements and measurements of parent volatiles in a statistically significant sample of comets for all dynamical classes. This will need to be combined with a detailed comparison between disc chemical models and solar system dynamical models before the data can be interpreted in terms of formation location and delivery of volatiles to the terrestrial planets.

Competing interests. I declare I have no competing interests.

Funding. This material is based upon work supported by the National Aeronautics and Space Administration through the NASA Astrobiology Institute under Cooperative Agreement no. NNA09DA77A issued through the Office of Space Science and by a grant from the National Science Foundation, AST 1413736.

References

1. Kronk GW. 1984 *Comets: a descriptive catalog*. New York, NY: Enslow.
2. Marsden BG. 1983 Comets in 1983. *Q. J. R. Astron. Soc.* **27**, 102–113.
3. Marsden BG. 1986 Comets in 1984. *Q. J. R. Astron. Soc.* **27**, 590–606.
4. Chambers GF. 1909 *The story of the comets, simply told for general readers*. Oxford, UK: Clarendon Press.
5. Lyttleton RA. 1948 On the origin of comets. *Mon. Not. R. Astron. Soc.* **108**, 465–475. (doi:10.1093/mnras/108.6.465)
6. Whipple FL. 1950 A comet model. I. The acceleration of Comet Encke. *Astrophys. J.* **111**, 375–394. (doi:10.1086/145272)
7. Oort JH. 1950 The structure of the cloud of comets surrounding the Solar System and a hypothesis concerning its origin. *Bull. Astron. Inst. Neth.* **11**, 91–110.
8. Biermann L. 1951 Kometenschweife und solare korpuskularstrahlung. *Z. Astrophys.* **29**, 274–286.
9. Alfven H. 1957 On the theory of comet tails. *Tellus* **9**, 92–96. (doi:10.3402/tellusa.v9i1.9064)
10. Biermann L, Brosowski B, Schmidt HU. 1967 The interactions of the solar wind with a comet. *Solar Phys.* **1**, 254–284. (doi:10.1007/BF00150860)
11. Finson MJ, Probstein RF. 1968 A theory of dust comets. I. Model and equations. *Astrophys. J.* **154**, 327–352. (doi:10.1086/149761)

12. Mizuno H. 1980 Formation of the giant planets. *Prog. Theor. Phys.* **64**, 544–557. (bdoi:10.1143/PTP.64.544)
13. Pollack J. 1984 Origin and history of the outer planets: theoretical models and observations. *Ann. Rev. Astron. Astrophys.* **22**, 389–424. (doi:10.1146/annurev.aa.22.090184.002133)
14. Chambers W. 1998 Making the terrestrial planets: N-body integrations of planetary embryos in three dimensions. *Icarus* **136**, 304–327. (doi:10.1006/icar.1998.6007)
15. Goldreich P, Lithwick Y, Re'em S. 2004 Final stages of planet formation. *Astrophys. J.* **614**, 497–507. (doi:10.1086/423612)
16. Duncan M, Levison H, Dones L. 2004 Dynamical evolution of ecliptic comets. In *Comets II* (eds MC Festou, HU Keller, HA Weaver), pp. 193–204. Tucson, AZ: University of Arizona Press.
17. Walsh KJ, Morbidelli A, Raymond SN, O'Brien DP, Mandell AM. 2011 A low mass for Mars from Jupiter's early gas-driven migration. *Nature* **475**, 206–209. (doi:10.1038/nature10201)
18. Tsiganis K, Gomes R, MOrbidelli A, Levison HF. 2005 Origin of the orbital architecture of the giant planets of the solar system. *Nature* **435**, 459–461. (doi:10.1038/nature03539)
19. Izidoro A, de Souza Torres K, Winter OC, Haghighipour N. 2013 A compound model for the origin of Earth's water. *Astrophs. J.* **767**, 54. (doi:10.1088/0004-637X/767/1/54)
20. Levison HF, Kretke KA, Duncan MJ. 2015 Growing the gas-giant planets by the gradual accumulation of pebbles. *Nature* **524**, 322–324. (doi:10.1038/nature14675)
21. Wurm K. 1934 Beitrag zur deutung der vorg ange in kometen. I. Mit 2 abbildungen. *Z. Astrophys.* **8**, 281–291.
22. Delsemme AH, Swings P. 1952 Hydrates de gaz dans les noyaux cometaires et les grains interstellaires. *Ann. d'Astrophys.* **15**, 1–6.
23. Cowan JJ, A'Hearn MF. 1979 Vaporization of comet nuclei: light curves and life times. *Moon Planets* **21**, 155–171. (doi:10.1007/BF00897085)
24. Meech KJ, Jewitt DC, Ricker G. 1986 Early photometry of comet P/Halley—development of the coma. *Icarus* **66**, 561–574. (doi:10.1016/0019-1035(86)90091-6)
25. Meech KJ, Svoren J. 2004 Using cometary activity to trace the physical and chemical evolution of cometary nuclei. In *Comets II* (eds MC Festou, HU Keller, HA Weaver), pp. 317–335. Tucson, AZ: University of Arizona Press.
26. Prialnik D. 1997 Modelling gas and dust release from Comet Hale-Bopp. *Earth Moon Planets* **77**, 223–230. (doi:10.1023/A:1006224000795)
27. Spohn T, Seiferlin K, Benkhoff J. 1989 Thermal conductivities and diffusitivities of porous ice samples at low pressures and temperatures and possible modes of heat transfer in near surface layers of comets. In *Proc. Int. Workshop on Physics and Mechanics of Cometary Materials* (eds J Hunt, T Guyeme), ESA SP-302, Noordwijk, The Netherlands, pp. 77–81.
28. Prialnik D, Benkhoff J, Podolak M. 2004 Modeling the structure and activity of comet nuclei. In *Comets II* (eds MC Festou, HU Keller, HA Weaver), pp. 359–387. Tucson, AZ: University of Arizona Press.
29. Biver N. 1997 Evolution of the outgassing of Comet Hale-Bopp (C/1995 O1) from radio observations. *Science* **275**, 1915–1918. (doi:10.1126/science.275.5308.1915)
30. Bockeleé-Morvan D, Crovisier J, Mumma MJ, Weaver HA. 2004 The composition of cometary volatiles. In *Comets II* (eds MC Festou, HU Keller, HA Weaver), pp. 391–423. Tucson, AZ: University of Arizona Press.
31. A'Hearn MF, Millis RL, Schleicher DG, Osip DJ, Birch PV. 1995 The ensemble properties of comets: results from narrowband photometry of 85 comets, 1976–1992. *Icarus* **118**, 223–270. (doi:10.1006/icar.1995.1190)
32. Cochran AL, Barker ES, Gray CL. 2012 Thirty years of cometary spectroscopy from McDonald observatory. *Icarus* **218**, 144–168. (doi:10.1016/j.icarus.2011.12.010)
33. Mumma MJ, Charnley SB. 2011 The chemical composition of comets—emerging taxonomies and natal heritage. *Ann. Rev. Astron. Astrophys.* **49**, 471–524. (doi:10.1146/annurev-astro-081309-130811)
34. DelloRusso N, Kawakita H, Vervack RJ, Weaver HA. 2016 Emerging trends and a comet taxonomy based on the volatile chemistry measured in thirty comets with high-resolution infrared spectroscopy between 1997 and 2013. *Icarus* **278**, 301–332. (doi:10.1016/j.icarus.2016.05.039)

35. Weissman PR, Asphaug E, Lowry SC. 2004 Structure and density of cometary nuclei. In *Comets II* (eds MC Festou, HU Keller, HA Weaver), pp. 337–357. Tucson, AZ: University of Arizona Press.
36. Britt DT *et al.* 2004 The morphology and surface processes of comet 19P/Borrelly. *Icarus* **167**, 45–53. (doi:10.1016/j.icarus.2003.09.004)
37. A'Hearn MF. 2011 Comets as building blocks. *Ann. Rev. Astron. Astrophys.* **49**, 281–299. (doi:10.1146/annurev-astro-081710-102506)
38. Belton MJS *et al.* 2007 The internal structure of Jupiter family cometary nuclei from Deep Impact observations: the 'talps' or 'layered pile' model. *Icarus* **187**, 332–344. (doi:10.1016/j.icarus.2006.09.005)
39. Meech KJ, Wilson L, Prialnik D. 2008 Smooth regions on comet 9P/Tempel 1: cryovolcanic emplacement? *Asteroids Comets Meteors.* LPI Contribution no. 1405, ID 8341.
40. Belton MJS, Melosh J. 2009 Fluidization and multiphase transport of particulate cometary material as an explanation of the smooth terrains and repetitive outbursts on 9P/Tempel 1. *Icarus* **200**, 280–291. (doi:10.1016/j.icarus.2008.11.012)
41. A'Hearn MF *et al.* 2011 EPOXI at comet Hartley 2. *Science* **332**, 1396–1400. (doi:10.1126/science.1204054)
42. Meech KJ *et al.* 2011 EPOXI: Comet 103P/Hartley 2 observations from a worldwide cammpaign. *Astrophys. J.* **734**, L1. (doi:10.1088/2041-8205/734/1/L1)
43. Meech KJ *et al.* 2013 Outgassing behavior of C/2012 S1 (ISON) from 2011 September to 2013 June. *Astrophys. J.* **776**, L20. (doi:10.1088/2041-8205/776/2/L20)
44. Snodgrass C, Tubiana C, Bramich DM, Meech K, Boehnhardt H, Barrera L. 2013 Beginning of activity in 67P/Churyumov-Gerasimenko and predictions for 2014–2015. *Astron. Astrophys.* **557**, A33. (doi:10.1051/0004-6361/201322020)
45. Belton MJS *et al.* 2013 The complex spin state of 103P/Hartley 2: kinematics and orientation in space. *Icarus* **22**, 595–609. (doi:10.1016/j.icarus.2012.06.037)
46. Gruen E. 1993 Development of a dust mantle on the surface of an insolated ice-dust mixture—results form the KOSI-9 experiment. *J. Geophys. Res.* **98**, 15091–15104. (doi:10.1029/93JE01134)
47. Bar-Nun A, Laufer D. 2003 First experimental studies of large samples of gas-laden amorphous 'cometary' ices. *Icarus* **161**, 157–163. (doi:10.1016/S0019-1035(02)00016-7)
48. Ootsubo T. 2012 Akari near-infrared spectroscopic survey for CO_2 in 18 comets. *Astrophys. J.* **752**, 15. (doi:10.1088/0004-637X/752/1/15)
49. Reach WT, Kelley MS, Vaubaillon J. 2013 Survey of cometary CO_2, CO, and particulate emissions using the *Spitzer* space telescope. *Icarus* **226**, 777–797. (doi:10.1016/j.icarus.2013.06.011)
50. Bauer JM *et al.* 2015 The NEOWISE-discovered comet population and the $CO + CO_2$ production rates. *Astrophs. J.* **814**, 85. (doi:10.1088/0004-637X/814/2/85)
51. A'Hearn MF *et al.* 2012 Cometary volatiles and the origin of comets. *Astrophys. J.* **758**, 29. (doi:10.1088/0004-637X/758/1/29)
52. Willacy K, Woods PM. 2009 Deuterium chemistry in protoplanetary disks. II. The inner 30 AU. *Astrophys. J.* **703**, 479–499. (doi:10.1088/0004-637X/703/1/479)
53. Fernandez YR *et al.* 2013 Thermal propoerties, sizes, and size distribution of Jupiter-family cometary nuclei. *Icarus* **226**, 1138–1170. (doi:10.1016/j.icarus.2013.07.021)
54. Li J-Y *et al.* 2013 Photometry properties of the nucleus of comet 103P/Hartley 2. *Icarus* **222**, 559–570. (doi:10.1016/j.icarus.2012.11.001)
55. Sunshine JM *et al.* 2006 Exposed water ice deposits on the surface of comet 9P/Tempel 1. *Science* **311**, 1453–1455. (doi:10.1126/science.1123632)
56. Lamy P, Toth I. 2009 The colors of coemtary nuclei—comparison with other primitive bodies of the Solar System and implications for their origin. *Icarus* **201**, 674–713. (doi:10.1016/j.icarus.2009.01.030)
57. Snodgrass C, Fitzsimmons A, Lowry SC, Weissman P. 2011 The size distribution of Jupiter family comet nuclei. *Mon. Not. R. Astron. Soc.* **414**, 458–469. (doi:10.1111/j.1365-2966.2011.18406.x)
58. McKeegan KD. 2011 The oxygen isotopic composition of the Sun inferred from captured solar wind. *Science* **332**, 1528–1532. (doi:10.1126/science.1204636)
59. Marty B. 2012 The origins and concentrations of water, carbon, nitrogen and noble gases on Earth. *Earth Planet. Sci. Lett.* **313–314**, 56–66. (doi:10.1016/j.epsl.2011.10.040)

60. Owen T, Bar-Nun A. 2001 Contributions of icy planetesimals to the Earth's early atmosphere. *Orig. Life Evol. Biosph.* **31**, 435–458. (doi:10.1023/A:1011809412925)
61. Hartogh P. 2011 Ocean-like water in the Jupiter-family comet 103P/Hartley 2. *Nature* **478**, 218–220. (doi:10.1038/nature10519)
62. Yurimoto H, Krot AN, Choi B-G, Aléon J, Kunihiro T, Brearley AJ. 2008 Oxygen isotopes of chondritic components. *Rev. Mineral. Geochem.* **68**, 141–186. (doi:10.2138/rmg.2008.68.8)
63. Lyons JR, Young ED. 2005 CO self shielding as the origin of oxygen isotope anomalies in the early solar nebula. *Nature* **435**, 317–320. (doi:10.1038/nature03557)
64. Owen T, Mahaffy PR, Niemann HB, Atreya S, Wong M. 2001 Protosolar nitrogen. *Astrophs. J.* **553**, L77–L79. (doi:10.1086/320501)
65. Bockelée-Morvan D *et al.* 2015 Cometary isotopic measurements. *Space Sci. Rev.* **197**, 47–83. (doi:10.1007/s11214-015-0156-9)
66. Wooden D. 2008 Cometary refractory grains: interstellar and nebular sources. *Space Sci. Rev.* **138**, 75–108. (doi:10.1007/s11214-008-9424-2)
67. Joswiak DJ, Brownlee DE, Matrajt GM. 2008 Mineralogical origins of Wild 2 comet particles collected by the Stardust spacecraft. *Geochim. Cosmochim. Acta* **72**, A441.
68. Brownlee DE, Joswiak D. 2016 The diversity of rocky materials in comets. American Astronomical Society DPS meeting no. 48, ID 308.01.
69. Lisse CM *et al.* 2006 Spitzer spectral observations of the deep impact ejecta. *Science* **313**, 635–640. (doi:10.1126/science.1124694)
70. A'Hearn MF *et al.* 2008 Deep Impact and sample return. *Earth Planets Space* **60**, 61–66. (doi:10.1186/BF03352762)
71. Paganini L, Mumma MJ, Villanueva GL, Keane JV, Blake GA, Bonev BP, DiSanti MA, Gibb EL, Meech KJ. 2014 C/2013 R1 (Lovejoy) at IR wavelengths and the variabiilty of CO abundances among Oort cloud comets. *Astrophys. J.* **791**, 122. (doi:10.1088/0004-637X/791/2/122)
72. Feldman PD, Festou MC, Tozzi GP, Weaver HA. 1997 The CO_2/CO abundance ratio in 1P/Halley and several other comets observed by IUE and HST. *Astrophys. J.* **475**, 829–834. (doi:10.1086/303553)
73. Jewitt D. 2012 The active asteroids. *Astron. J.* **143**, 66. (doi:10.1088/0004-6256/143/3/66)
74. Hsieh HH. 2017 Asteroid–comet continuum objects in the solar system. *Phil. Trans. R. Soc. A* **375**, 20160259. (doi:10.1098/rsta.2016.0259)
75. Hsieh HH, Jewitt D. 2006 A population of comets in the main asteroid belt. *Science* **312**, 561–563. (doi:10.1126/science.1125150)
76. Meech KJ, Yang B, Keane J, Hainaut O, Kleyna J, Hsieh H, Bauer J, Wainscoat R, Veres P. 2014 C/2013 P2 Pan-STARRS—the Manx comet. American Astronomical Society DPS meeting no. 46, ID 200.02.
77. Meech KJ, Yang B, Kleyna J, Hainaut OR, Svetlana B, Keane JV, Micheli M, Morbidelli A, Wainscoat RJ. 2016 Inner solar system material discovered in the Oort cloud. *Sci. Adv.* **2**, e1600038. (doi:10.1126/sciadv.1600038)